



Development of IASI Outgoing Longwave Radiation Algorithm

Hai-Tien Lee⁽¹⁾, Robert G. Ellingson⁽²⁾, Arnold Gruber⁽¹⁾

⁽¹⁾ University of Maryland, College Park, Maryland, USA ⁽²⁾ Florida State University, Tallahassee, Florida, USA



INTRODUCTION

The earth radiation budget at the top of the atmosphere describes the state of balance of the incoming solar radiation, the reflected solar radiation and the thermal emission by the earth-atmosphere system. The surplus/deficit of the earth radiation budget is one of the main driving forces that define earth's climate. Its importance has been long recognized and the observation of these parameters has been continuously pursued since the inception of the meteorological satellites.

In the past three decades, dedicated missions/instruments for earth radiation budget measurements have been conducted that produced data of various lengths, including the Earth Radiation Budget Experiment (ERBE) onboard NIMBUS-7 (launched in 1978), the Earth Radiation Budget Experiment (ERBE) onboard NOAA-9/10/ERBS (1985), the Scanner for Radiation Budget (ScaRaB) onboard Meteor-3/7 (1994), the Cloud and the Earth's Radiant Energy System (CERES) onboard TRMM, Terra and Aqua satellites (1998), and the Geostationary Earth Radiation Budget (GERB) onboard Meteosat-8/9/10 (2004). The CERES and GERB continue to operate.

For climate change studies, discontinuities are a haunting problem for any data set including those derived from those missions because it can cause large uncertainties in time series analysis. To complement this deficiency, one can estimate the radiative fluxes using observations available on the operational weather satellites, e.g., the NOAA Polar Environmental Satellites (POES) that provide continuous observations for the past three decades from nearly identical instruments.

The HIRS outgoing longwave radiation (OLR) climate data set (CDR) has been derived with the HIRS radiance observations from NOAA TIROS-N series and MetOp satellites from 1979 to the present (Lee et al., 2007). The multi-spectral OLR estimation algorithm developed by Ellingson et al. (1989) provides a fairly accurate and robust method that estimates OLR directly from radiance observations from HIRS or other sounding instruments. The employment of the inter-satellite calibration and regional/monthly OLR diurnal models further improved the homogeneity and continuity of this climate data set. The HIRS OLR agrees with CERES OLR with absolute accuracy within 2 Wm^{-2} at a precision of about 4 Wm^{-2} . Most importantly, the stability of HIRS OLR time series is comparable to that of the ERBS Non-scanner OLR time series, which is about 0.3 Wm^{-2} per decade.

At this quality, the HIRS OLR CDR is the longest OLR time series available so far. It is in our best interest to extend this OLR time series by developing consistent OLR algorithms for the follow-up operational sounding instruments, including the Infrared Atmospheric Sounding Interferometer (IASI) flown on the MetOp and the Cross-track Infrared Sounder (CrIS) planned for the NPOESS, as HIRS is toward its end (last one on MetOp-B).

This poster describes the basic approaches of the IASI OLR algorithm development and preliminary assessments on its performance.

IASI Instrument Spec

- The Infrared Atmospheric Sounding Interferometer (IASI) is composed of a Fourier transform spectrometer and an associated Integrated Imaging Subsystem (IIS)
- Three bands between 645 cm^{-1} and 2760 cm^{-1} (15.5 and $3.63 \mu\text{m}$), with a spectral resolution of 0.5 cm^{-1} (FWHM) after apodisation (LTC spectra). (The spectral sampling interval is 0.25 cm^{-1} .)

Band	Wavenumbers (cm^{-1})	Wavelength (μm)
1	645 – 1210	8.26 – 15.50
2	1210 – 2000	5.00 – 8.26
3	2000 – 2760	3.62 – 5.00

- Radiance data: Level 1C calibrated apodized radiance spectra with geolocation and time stamp information at the Effective FOV (EFOV) composed of 2x2 Instantaneous FOV (IFOV) @ 12 km at nadir.

Acknowledgments

Thank Jiajing Gu for performing LBLRTM simulations; Tim Hultberg for providing Eumetsat principle component compression (PCC) database; Chris Barnert for providing NESDIS PCC and many helpful discussions; NOAA NCDC for providing IASI Level 1C data; NASA LaRC Atmospheric Science Data Center for providing CERES data. This research is in part supported by the NOAA Climate Program Office Scientific Data Stewardship Program.

References

- Ellingson, R. G., D. J. Yanuk, H.-T. Lee and A. Gruber, 1989: A technique for estimating outgoing longwave radiation from HIRS radiance observations. *J. Atmos. Ocean. Tech.*, **6**, 706-711.
- Lee, H.-T., A. Gruber, R. G. Ellingson and I. Laszlo, 2007: Development of the HIRS Outgoing Longwave Radiation climate data set. *J. Atmos. Ocean. Tech.*, **24**, 2029-2047.
- Loeb, N. G., et al., 2001: Determination of Unfiltered Radiances from the Clouds and the Earth's Radiant Energy System Instrument. *J. Applied Meteor.*, **40**, 822-835.

OLR Observation and OLR Estimation

Broadband OLR Observation

The outgoing longwave radiation (OLR) is the integral of the TOA upward specific intensity over frequency and solid angle domains,

$$OLR = \int_0^{2\pi} \int_0^\pi \int_0^\infty I_\nu(z; \mu, \phi) \mu d\mu d\phi d\nu$$

$I_\nu(z; \mu, \phi)$ is TOA upward LW specific intensity at wavenumber ν , azimuth angle ϕ and local zenith angle θ . Whereas $\mu = \cos(\theta)$

While the OLR is usually not observable over these integrals entirely, the measurement of OLR requires two steps of conversions, in frequency and in solid angle:

- In CERES, the **LW Radiance L** is first obtained by the unfiltering process (Loeb et al., 2001) to account for the spectral responses, where an error of $\sim 0.1\%$ std (or $\sim 0.3 \text{ Wm}^{-2}$ equivalent flux) is introduced. Secondly, the hemispheric solid angle integral for OLR is performed with the angular directional models (ADM) parameterized as functions of atmospheric state S and observing geometry.

$$L(\mu, \phi) = \int_0^{2\pi} \int_0^\pi I_\nu(z; \mu, \phi) d\nu \Rightarrow OLR = \int_0^{2\pi} \int_0^\pi L(\mu, \phi) \mu d\mu d\phi = \frac{L(\mu, \phi)}{ADM(S; \mu, \phi)}$$

HIRS OLR

Ellingson et al. (1989) developed an OLR estimation method using the narrowband radiance observations from the High-resolution Infrared Sounder (HIRS). The multi-spectral OLR algorithm expressed the OLR as a linear combination of the radiances N_i at selected channel i , observed from a local zenith angle θ :

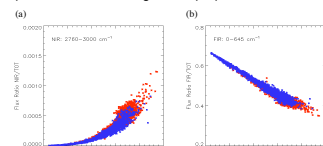
$$OLR = a_0(\theta) + \sum_{i=1}^N a_i(\theta) N_i(\theta)$$

The channel selections for the HIRS OLR retrieval are: HIRS/2: Channels 3, 7, 10, 12; HIRS/21,3,4: Channels 3, 10, 11, 12.

Note that the HIRS OLR algorithm is designed to handle the narrow-to-broadband conversion (spectral integral) and solid angle integral in one step.

IASI OLR

IASI radiance observation covers a very wide and continuous spectral range, from 645 to 2760 cm^{-1} . The total radiance in that frequency range can be obtained by direct summation. However, the un-observed spectra still remain a significant proportion of the total LW energy, about 40-60%.

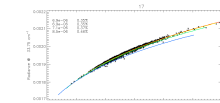


The fraction of the LW energy that is not directly observed by IASI radiance observations in spectral ranges (a) near IR $2760\text{--}3000 \text{ cm}^{-1}$, and (b) far IR $0\text{--}645 \text{ cm}^{-1}$.

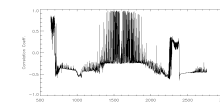
About 40 to 60% of LW energy in the far IR is not directly observed by IASI that needs to be estimated.

Red: clear sky, Blue: cloudy sky conditions.

The un-observed LW spectrum and the radiance at other frequencies are governed by the same physical laws that their variances can be explained by those with similar absorption properties.

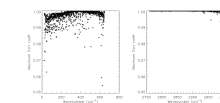


This example shows the relationship between the radiances at wavenumber 34 and 2091 cm^{-1} . The scatter points and the red fitting curve is for the zenith angle 0° condition, whereas the yellow, green and blue fitting curves (whose corresponding points are not shown) are for zenith angles 21.48 , 47.93 , and 70.73° , respectively. The log-log fit produces relative rms errors at about 0.4% for all angles.



This plot shows the linear correlation between the radiance at 25 cm^{-1} and the radiances in 645 to 2760 cm^{-1} observable by IASI.

The best correlated radiance is selected as the predictor to estimate the radiance in the un-observed part of the spectrum, thus, a full spectrum can be constructed.



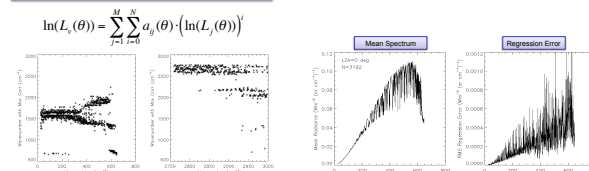
The maximum correlation coefficients found for the radiances in the un-observed spectra, the far IR (left) and near IR (right), with a radiance available in IASI spectral range.

Note the strong correlations shown among the radiance spectrum – over 0.99 for most far IR, and nearly perfect correlations for the near IR.

Formulation of IASI OLR Model

A database of radiance (from 25 to 3000 cm^{-1} at 0.5 cm^{-1} resolution) and flux of 3200 cases were calculated using the LBLRTM model and Phillips Soundings following HIRS OLR simulation procedures (Jiujing Gu). Two forms of IASI OLR model were constructed:

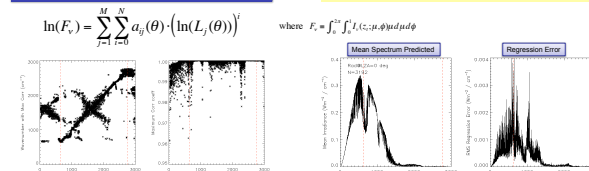
Spectral Radiance Estimation



The best predictor is found with the highest correlation between radiances, in log-log transformation in this case. Every "un-observed" radiance L_ν (located in x-axis) is paired with a radiance predictor L_ν (located in y-axis) to achieve best estimation. Left: for far IR region; Right: for near IR region.

Spectral radiance estimation errors (regression rms errors) for the far IR $25\text{--}645 \text{ cm}^{-1}$ region (right panel). The mean radiance spectrum is shown for reference (left). Model parameter setting is M=1, N=1 for this test. For the full LW spectrum construction purpose, the rms errors is $\sim 0.15\%$ of the unobserved spectrum, or, $\sim 0.2 \text{ Wm}^{-2}$ equivalent flux. Some temperature dependency was seen in the cold cloudy conditions.

Spectral Flux Estimation



For the spectral flux F_ν at wavenumber ν (x-axis), the radiance predictor L_ν at zenith angle θ (y-axis) is the one with the highest correlation (in log-log transformation). Left: The wavenumber of the selected radiance predictors and their corresponding correlation coefficients (right).

Right: Spectral flux estimation errors (regression rms errors). Left: The mean spectral flux. Model parameters M=1, N=2 for $\theta=0^\circ$ case. The regression rms error is $\sim 0.2 \text{ Wm}^{-2}$ for OLR estimation. Some scene dependency in warmer cases is noticed in the residual distribution.

Discussions and Future Works

Two forms of IASI OLR estimation model are presented, both showed very high accuracy.

The spectral radiance model estimates the un-observed spectra; re-constructing the full LW radiance spectrum which can be summed to equivalence the unfiltered radiance derived from broadband observation at comparable accuracy. The rms errors for spectrum reconstruction is $\sim 0.2 \text{ Wm}^{-2}$, comparable to that of the CERES spectrum unfiltering error of $\sim 0.1\%$ std (or $\sim 0.3 \text{ Wm}^{-2}$ equivalent flux).

The spectral flux model produces the flux spectrum that, similar to HIRS OLR algorithm, can estimate OLR directly with a regression rms error of $\sim 0.2 \text{ Wm}^{-2}$ when summed.

Accuracy may be further improved with refined model formulation discriminating strong/weak absorptions and/or with expanded model size.

Principle Component Compression (PCC)

- Investigate the IASI OLR model using principle components as predictors (PCC from Eumetsat vs NESDIS)
- PCC vs Radiance Tradeoff:
 - Pros: Large reduction of data volume and noise filtering. Approximately 50 PC.
 - Cons: Introducing reconstruction error

LW Radiance/Flux Validation

- Validation of IASI OLR models to be performed with co-located IASI and CERES instantaneous observations.
 - Radiance validation: Compare IASI estimated radiance with CERES unfiltered radiance
 - Flux validation: Compare IASI estimated OLR with CERES SSF LW flux